In: Laser Keratectomy: Approaches, Complications...
Author: Luis W. Schröder and Felix J. Walter

ISBN 978-1-60456-863-9

Short Communication B

Excimer Laser Surgery: A Watchful Eye for the Future

Marco Lombardo[*1,2], *Maria Penelope De Santo* [2], *Giuseppe Lombardo* [1,2], *Riccardo Barberi* [2], *Lucia Ziccardi* [3], *and Sebastiano Serrao* [3]

[1] Vision Engineering, Reggio Calabria and Rome, Italy
[2]INFM-CNR LiCryL Laboratory, Physics Department, University of Calabria, Arcavacata di Rende (CS), Italy
[3]Serraolaser, Rome, Italy

Abstract

Excimer laser corneal surgery allows the precise removal of tissue and it is nowadays used worldwide for the correction of the eye's optical aberrations. During the last years, novel methods and techniques have been developed in order to improve the accuracy of surface ablation surgery. On the other hand, even in an era of high-precision treatment algorithms, discrepancies between the intended and realized visual outcomes are sometimes manifest. The biophysical responses of the cornea undermine the predictability and stability of refractive surgery and contribute to these discrepancies.

Numerous factors depending on the ablation parameters may vary the remodeling of the ablated corneal surface leading to abnormal wound healing. A smooth postoperative stromal surface is required to achieve a high-quality visual outcome. In this work, we provide nanometer-resolved images of either native or photoablated corneas to demonstrate the opportunity in which Atomic Force Microscopy (AFM) may be valuable to understand the laser-tissue interaction and characterize the three-dimensional ultra-structural changes of the corneal stroma induced by excimer laser surgery.

The stromal surface of eight porcine corneas, both natural and photoablated, was imaged with AFM operating in balanced salt solution and contact mode. The AFM images of the intact corneal stroma, exposed after chemical removal of the epithelium,

* Address correspondence to: Dr. Marco Lombardo, MD, PhD, via Adda, 7 – 00198, Rome – ITALY, Phone and Fax: +39 06 88 40 971, E-mail: mlombardo@visioeng.it

showed a smooth surface with pores of varying diameter and dimension consisting in the Bowman's layer. Following ablation, the stromal surface showed undulations and micro-granular structures. These structures are considered to be either collapsed collagen fibrils and debris, directly due to the effects of laser beam impact onto the stromal surface. Topographical data, calculated using the section analysis module of the AFM software, showed an increased roughness of the post-ablated stromal surface compared to its native state, with a mean *root mean square roughness* value of 215 ± 49 nanometer (nm) and 144 ± 41 nm respectively. Nevertheless, the quantitative analysis proved that the laser cut of commercial excimer laser systems is very precise in removing even infinitesimally small amounts of tissue.

Introduction

Excimer laser corneal surgery has become one of the most widely employed surgical techniques in Ophthalmology. Photorefractive surgery, by means of a 193 nm wavelength laser beam generated by a gas mixture of Argon and Fluorine (ArF), remodels the profile of the cornea and minimizes the refractive defects of the eye. The laser by its impact on the corneal plane breaks, through a photochemical interaction termed *photoablation*, the covalent organic bonds of the stromal collagen fibers, hence removing the corneal tissue with extreme precision. Different techniques for reshaping the corneal profile are used worldwide, as photorefractive keratectomy (PRK), laser epithelial keratomileusis (LASEK), laser assisted in situ keratomileusis (LASIK) [1] and epi-LASIK [2].

During the last decade, photorefractive surgery has undergone rapid technological development. The individualized correction of the eye optical aberrations will be the next golden standard of refractive surgery allowing all the patients treated to achieve their optimal individual visual perception. Customized ablation, linking the measurement of ocular wavefront aberrations and treatment, aims to eliminate low-order ocular aberrations, i.e., the sphero-cylindrical errors, whilst minimizing high-order aberrations [3,4,5].

On the other hand, the ultimate visual outcome of excimer laser refractive surgery depends on the biophysical response of the corneal tissue, that definitely represents the limiting factor for this type of surgery [6]. The biomechanical changes of the cornea induced by ablation and the epithelial and stromal healing are the two biophysical issues involved in the variability of the individual response to laser surgery. It is well known that the final corneal profile, and thus the corneal optical quality, after surgical reshaping of the cornea is a function of the biomechanical response of the tissue to a change in its structure. Predicting the biomechanical response is one of the major challenges of customized, aberration-reducing ablative procedures [7]. In addition, it is widely held that a smooth post-ablation surface is mandatory if refractive surgery is to be considered effective: an abnormal epithelial-stromal reaction of the ablated cornea is the consequence of an imperfectly polished ablated surface [8]. A smooth stromal surface is at the basis of an improved refractive result and it is associated with an increased predictability and stability of the final visual outcome [9]. Also, the more the postoperative corneal surface micrometric irregularities, the greater will the amount of induced high-order aberrations be [10], thus resulting in a decrease of visual performance.

The goal of research in this setting is to improve outcomes and reduce complications by discerning details of the biophysical pathways, identifying measurable predictors of individual responses and developing appropriate models for controlling or compensating for these factors.

A complete and correct knowledge of the ultra-structure of the photoablated corneal surface will allow ophthalmic surgeons and laser manufacturers to better test the ablation parameters and consequently improve the effectiveness of future customized refractive surgery [11,12].

The aim of the present study is to examine the effect of excimer laser treatment on porcine corneas using Atomic Force Microscopy (AFM) [13] and display the three dimensional characteristics of the ablated surface with respect to the natural one.

Materials and Methods

Eight enucleated porcine fresh eye globes were used for this study, half of which underwent photorefractive keratectomy (PRK). Ablations of specimens were performed using the Technolas Keracor 217C excimer laser (Bausch and Lomb, Dornach, Germany). A laser technique was employed to excise the corneal epithelium [14] and then an ablation zone of 4.00 mm in diameter with a maximum depth of 80 micron (μm) was performed [15,16,17,18]. The non ablated porcine eyes were incubated in the presence of EDTA (2.5 mM) for 2 hours and the epithelium was then gently removed in order to expose the native anterior stromal surface.

The corneal surface was washed with a jet of saline solution prior to fixation and then all the corneal specimens, both natural as well as photoablated, were immediately fixed in situ by topical application and anterior chamber injection of a 2.5% glutaraldehyde solution [19]. All the eyes were conserved at a temperature of 4°C for 24 hours in the glutaraldehyde solution. Previous works [20,21] stated that the fixation procedure we used does not alter the surface of specimens compared to fresh unprepared ones and also facilitates the acquisition of high-resolution images. Therefore, the corneas were excised using a Hessburg-Barron trephine in order to obtain corneal specimens with a diameter of 8.00 mm. This procedure minimizes any possible alteration in the structure of the specimens themselves [22]. All the specimens were placed on the microscope sample holder and glued with cyanoacrylate glue with the endothelial side facing downwards. Maximum attention was paid during these maneuvers not to damage the corneal surface.

As group of control, we analyzed with AFM four human hairs either intact or after photoablation of exposed regions using a custom aluminum mask. A maximum ablation depth of 60 μm has been performed. The hairs were glued at the edges, paying maximum care in order not to deform their biological structure, on the sample holder.

Atomic Force Microscopy allows a three-dimensional (3-D) topographic reconstruction of the investigated sample on a nanometric scale (Figure 1). A commercially available Atomic Force Microscope (Autoprobe CP, Veeco, Sunnyvale, CA) was operated in balanced salt solution (BSS) in contact operating mode [15,16,18], using a V-shaped silicon nitride gold coated cantilever with a spring constant of 0.01 N/m (Veeco Metrology Group,

Sunnyvale, CA). The vertical resolution of the instrument is in the order of 0.1 nm. All the reported images were acquired with a 256 x 256 points resolution with scan rates of 1 to 5 Hz per line.

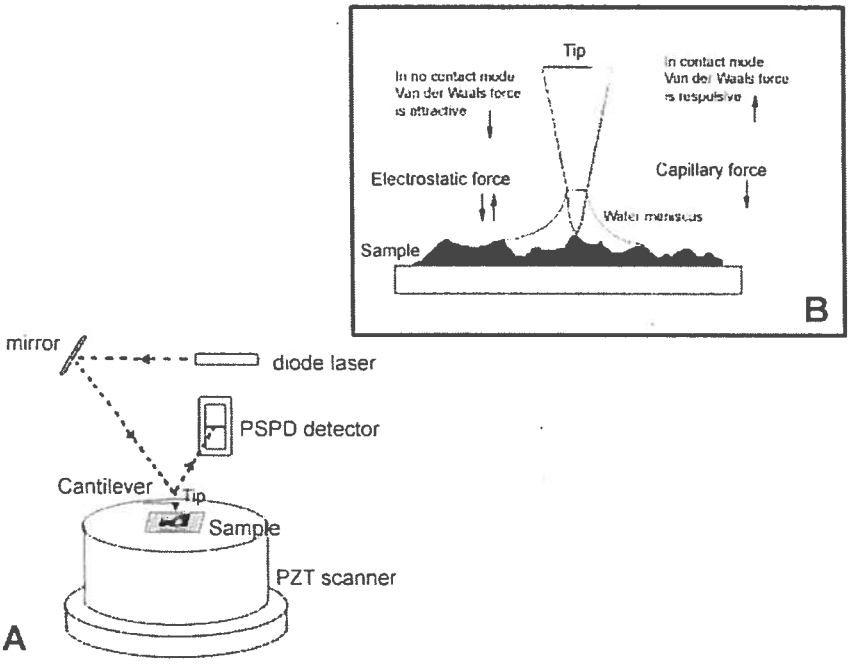

Figure 1. A) In AFM, the sample is scanned by a tip which is mounted on a flexible cantilever. While scanning, the forces between the tip and the sample cause bending of the cantilever. The deflection is monitored through an optical system, consisting of a laser diode and a position sensitive photo-detector (PSPD). The laser beam hits the reflective back of the cantilever and is reflected in the two-segmented photodiode. The PSPD itself permits a light displacement resolution less than one nm. The topography of the sample is obtained by plotting the deflections of the cantilever as a function of its position on the sample. With an appropriate feedback system, the deflection of the cantilever can be kept constant while the tip scans the specimen. During measurement, the specimen is driven by a piezoelectric scanner under the tip.

B) Several forces typically contribute to the deflection of the cantilever. The force most commonly associated with atomic force microscopy is an interatomic force called the Van der Waals force, the magnitude of which is in the range of nanoNewton (nN). Electrostatic forces and capillary forces between the tip and the sample are also involved.

An AFM may operate in contact or in no-contact mode. When the microscope operates in contact mode the tip scans the sample in close contact (a few Ångstroms) with the surface. The force on the tip is repulsive and has a magnitude of 10^{-7}-10^{-6} Newton (N). In no-contact mode, the tip is held at about one hundred Ångstroms from the surfaces. Hence, the forces between the tip and the sample are weaker than the ones in contact mode and approximate 10^{-12} N.

A single area on the cornea was imaged twice obtaining the same results, in order to ensure that the force exerted was not sufficient to damage the sample surface causing artifacts. Multiple imaging techniques were used to minimize the possibility that artifacts

introduced by fixation could be misinterpreted as surface features. High-quality images were obtained within a wide range of image magnification. On the other hand, the area scanned was limited to a maximum of 50 μm^2 owing to the gross curvature of the cornea.

Table 1. Average (± SD) quantitative analysis of the surface roughness of eight porcine corneas by means of RMS roughness value within a 10 μm^2 reference surface area

	RMS *roughness* (nanometer, M ± SD)*
Native Stroma (exposed Bowman's layer; 4 samples)	144 ± 41 nm
Ablated stroma (4 samples)	215 ± 49 nm

* Student's *t*-test: $P<.05$.

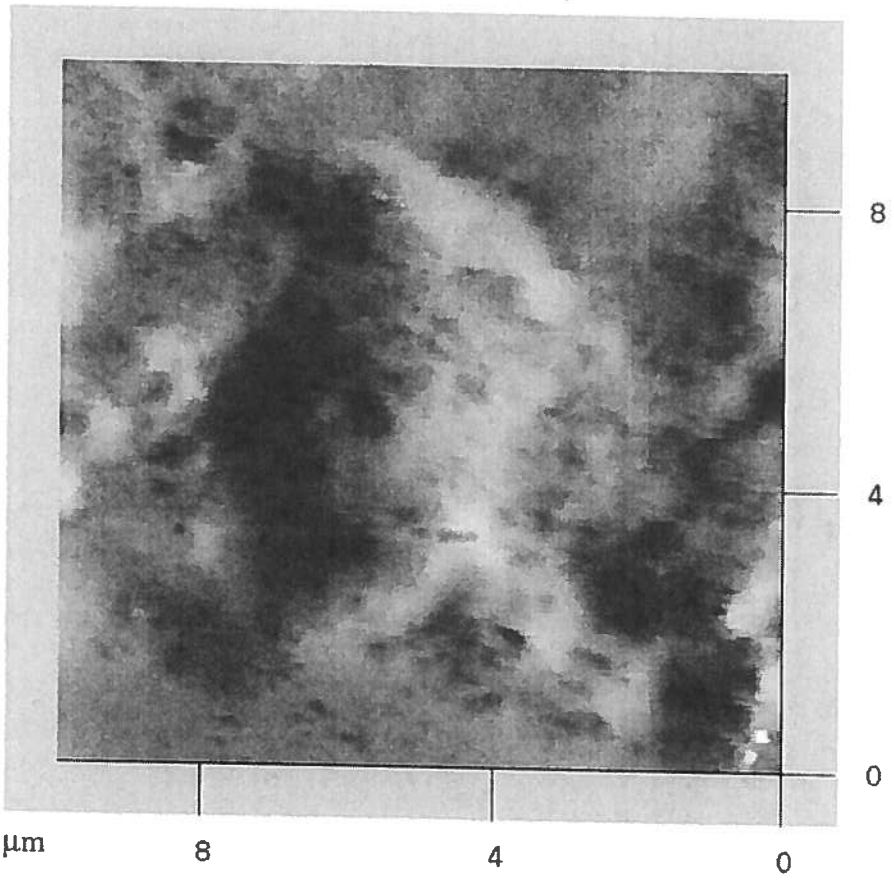

Figure 2. AFM image of the Bowman's layer. The Bowman's layer shows a complex topography of pores of varying sizes. Note the felt-like architecture of the surface. This complex topography provides an interface for cell-substratum interaction, it may also allow for the diffusion of components or for the passage of the nerves into the overlying epithelial layers. In the map, black corresponds to low features and white to high features (image size: 10 x 10 µm).

A set of images were taken from different areas close to the center of the corneal surface of the single specimen, both for the original and photoablated corneas.

All the images used for roughness measurement were processed using the specific AFM software. Processing included only flattening (2^{nd} order) to remove the background slope due to the nonlinearities of the piezoelectric AFM scanner. Moreover, profile measurements and quantitative characterization of the surface roughness were achieved again using the AFM software. This allows measurements of linear distance and selection of one or more sections of the image for region analysis. Surface roughness measurements were made by calculating the root mean square value of the roughness within the given area (RMS roughness), i.e., the standard deviation of the height data. The surface roughness of the corneal stroma was evaluated by calculating the RMS roughness on reference surface areas of 10 μm^2. The same procedure was followed for the analysis of hairs. The Student's paired *t*-test was used to compare the differences in *RMS roughness* values between native and photoablated surfaces. A *P* value less than 0.05 was considered statistically significant.

Results

Observation of the untreated corneas revealed a porous surface with pores of different depth and diameter, consisting in the Bowman's layer (Figure 2). The quantitative analysis of the Bowman's layer revealed a very smooth surface, as summarized in table 1.

The laser light output was the same we are used to set in clinical procedures, with fluence 120 mJ/cm^2, ablation rate 0.25 μm per pulse and the repetition rate 50 Hz. We selected the depth of ablation (80 μm and 60 μm for corneal specimens and hairs respectively) on the basis of the literature which proved that deeper treatments give rise to high surface irregularities [13,14,15,16].

Following ablation, the corneal surface was relatively rough showing undulations and micro-granular structures (Figure 3). Collagen fibrils arrangement areas were randomly displayed between these features that could represent the *pseudo-membrane* reported in scanning electron microscopy (SEM) studies [23]. The topographical analysis of the photoablated corneal specimens (the roughness measurements were performed on 50 areas of 10 μm^2 for statistical purpose) showed a significant increase ($P<.05$) in the surface roughness values in compare with the non ablated specimens.

AFM showed the hair cuticle consisting of scales of keratin lamellae. AFM images also clearly showed the longitudinal striations on the surface of the original hair's cuticle (Figure 4). The hair surface was very smooth along the non-ablated zones [24]. On the other hand, the ablated zones showed a diffuse granular topography at various magnification scales, probably due to the thermal effect generated by the ArF irradiation (Figure 5). The analysis has been performed on 50 areas of 10 μm^2. Results of the topographical analysis are summarized in Table 2. No significant differences ($P>.05$) between native and photoablated hairs' regions have been measured.

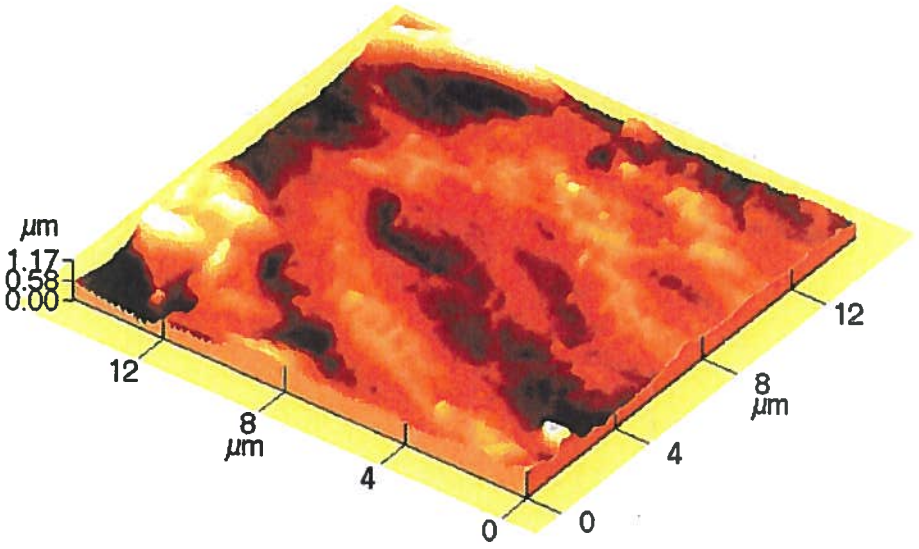

Figure 3. Three-dimensional view produced by AFM from the corneal stromal surface after standard eight diopters (maximum depth of ablation: 80 µm) photorefractive keratectomy. The image clearly shows undulations and granules as a result of the photoablative effect of the excimer laser at nano scale observation. Collagen fibrils are displayed between these features. Image size: 15 x 15 µm.

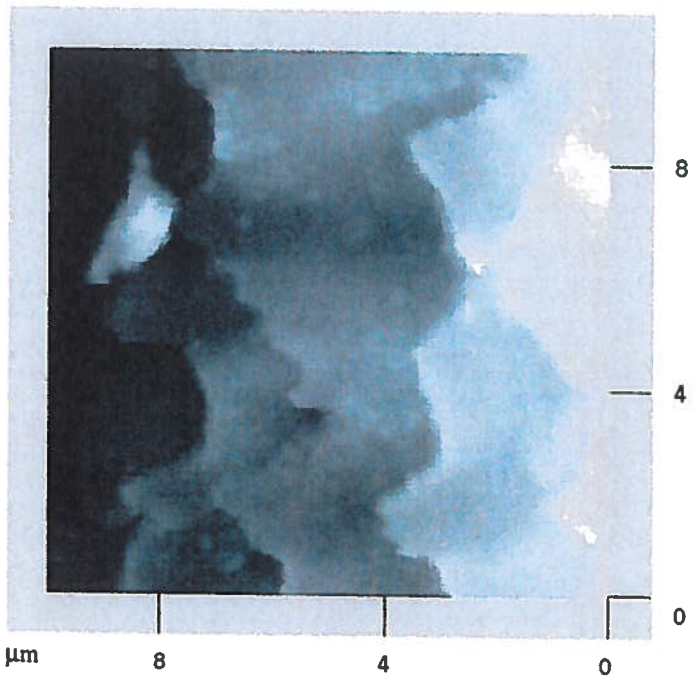

Figure 4. A three-dimensional AFM image of a natural human hair is shown. The surface appears to be very smooth. The steps correspond to the cuticular edges. Image size: 10 x 10 µm.

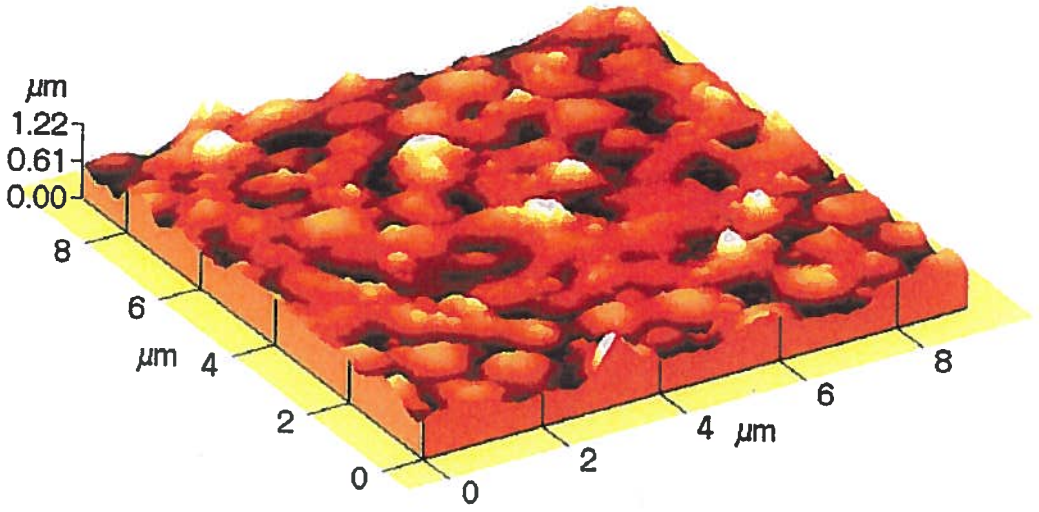

Figure 5. AFM three-dimensional image of a human hair after 60 µm depth photoablation. The sample surface shows a diffuse granular structure. These features may be directly dependent on the radiant and thermal effects of excimer laser onto the tissue. Image size: 10 µm x 10 µm.

TABLE 2. Average (± SD) quantitative analysis of the surface roughness of four human hairs by means of RMS roughness value within a 10 µm² reference surface area

	RMS *roughness* (nanometer, M ± SD)[†]
Non ablated hair (2 samples)	68 ± 37 nm
Ablated hair (2 samples)	82 ± 34 nm

[†] Student's *t*-test: $P>.05$.

Conclusion

During the last decade, photorefractive surgery has dramatically evolved with the simultaneous development of more accurate laser platforms and diagnostic instruments, such as corneal topographers or ocular wavefront sensors. The development of videokeratoscopes, capable of recording the corneal shape in detail, and aberrometers, that measure the eye's wave aberration, has revealed that although standard laser refractive surgery eliminates conventional refractive errors, high-order errors are typically induced [25].

A better understanding of the biophysical properties of the corneal tissue may allow the prediction and modulation of its response to laser ablation for more precise correction; for that reason, it is required a detailed analysis of either the biomechanical or epithelial/stromal postoperative remodeling of the cornea.

A smooth post-ablation surface is the principal issue to prevent an abnormal remodeling of the ablated tissue [26,27]. The more are the surface architectural irregular modifications induced by the ablation the more delayed will the wound healing be. This phenomenon leads to an irregular remodeling of both the epithelium and stroma and consequently to an increase in the amount of postoperative high-order aberrations. An uniform distribution intensity of the laser beam over the entire treatment zone is the first essential requirement to achieve a quite smooth ablated surface. Numerous factors depending on the ablation parameters may vary the remodeling of the ablated corneal surface: i.e., the homogeneity of the laser impulse, which must pass through a long optic route within the laser cavity and resist the variable conditions of humidity and temperature within the operating theatre before impacting onto the corneal plane [28]; the overlapping of the laser impulses until the complete removal of the predicted amount of corneal tissue has been achieved; the ejected molecular ablated debris deposited back onto the corneal surface and the adsorption of the UV excimer laser beam in the plume as a consequence of the corneal ablation [28]; the not negligible thermal effect, associated with laser photoablation, due to temperature higher than 40°C, at which the collagen fibers of the corneal stroma are denatured [29]; the inclination of the ocular plane [11] and the saccadic movements of the eye.

Since the publication of the first article on photorefractive surgery by S. Trokel et al. in 1983 [30], numerous experimental and clinical studies documenting the efficacy and safety of excimer laser surgery and the ultramicroscopic characteristics of the corneal surface on which excimer laser ablation had been performed, have been published [10,12,14,16,18,23]. However, a systematic approach to the physical phenomena and especially to the laser-tissue interaction is lacking in the literature. Many authors involved in the investigation of the excimer laser-related phenomena have performed experimental studies ablating different biological tissues [12,15,16,30]; this, in order to compare and validate the dependence of the changes occurring on the ablated corneas to the ablation parameters.

In this work, we investigated the smoothness and the sub-microscopic topographic characteristics of corneal specimens using a nano-resolved imaging technique, namely Atomic Force Microscopy.

AFM techniques allow the examination of biological samples with minimal preparation and hence with a low risk of altering the surface details [31,32]. Moreover, a nanometer resolved imaging of the three dimensional topography of ablated surfaces may yield valuable information about the influence of laser beams on tissues. Human hairs were also analyzed before and after photoablation; this in order to compare the impact of excimer laser on different soft biological tissues. The choice to examine the hair has been based on its physical properties, similar to those of the corneal tissue, constituted by regular overlapping lamellae of protein macromolecules and a smooth surface profile. Such a surface allowed us to demonstrate the accuracy of the laser beam reshaping and also to measure, on a nanometric scale, the irregularities induced by photoablation.

The proper method of imaging the corneal surface was determined by reviewing the literature [15,16,18,20] and based on results of our previous experiments [12, 33]: the AFM was operated in contact mode in BSS, using triangular cantilevers with a very low elastic constant.

AFM imaging of the untreated stromal surface revealed a smooth layer, with micro depressions of varying depth and dimensions. These features are considered to be the pores of the Bowman's layer which have been observed at SEM [34]. To date, only one work reporting similar observations made at AFM has been published in the literature [15]. The significance of the pores could be twofold: they could constitute the site through which nerve fibers pass [35], or else a sort of anchoring structure which helps epithelial cells to migrate [36]. The Bowman's layer is the natural plane on which the epithelial cells migrate and stratify, hence it has been hypothesized that a smooth and regular surface may favor the natural healing process of the corneal epithelium [36].

Images acquired following photoablation revealed micro irregularities on the exposed stroma. The changes occurring in the topography of the corneal plane after photoablation may be directly due to the effects of the laser beam impact onto the surface: the *pseudo-membrane* is considered to be a thin superficial zone of damage specific to 193-nm ArF laser irradiations that results in coagulation of the collagen fibrils [29,37,38]. The granular structures are considered to be either collapsed collagen fibrils and debris [12,16,17]. Additionally, authors have demonstrated that fragments of materials, induced by boiling water solutions of the tissue during ablation, are ejected from the ablated surface into the gaseous state, meaning that a thermal loading is produced during the photorefractive procedure [39]. Undulations and granules observed at nano-scale images are not to be related to the irregular overlapping of the laser impulses that becomes more important at the lower magnification scale imaging obtained with wave optics microscopic techniques.

The photoablated hair showed a nano-surface topography similar to that noticed in the corneal specimens, with undulations and granules, likely due to a similar thermal effect on either keratin or collagen macromolecules. Differences in the granular appearance and induced surface roughness between the ablated surface of the hairs and that of the corneas may be related to the lesser water content [40] and the different mechanical properties of keratinous tissues compared to collagenous tissues.

In conclusion, in this work, we reported nanometric changes in the three dimensional topographic architecture of the ablated stroma and an increased surface roughness in all the ablated specimens. Nevertheless, the quantitative analysis confirmed the precision of commercial excimer laser devices in removing infinitesimally small amounts of tissue.

Research efforts are ongoing to understand the laser-corneal tissue interaction and also predict and modulate the epithelial and stromal healing in order to optimize refractive and visual outcomes of laser refractive surgery. Novel methods and techniques are regularly developed in order to improve the accuracy of surface ablation surgery, as, for example, advanced surface ablation (ASA) procedures [9,12, 41].

References

[1] Munnerlyn CR, Koons SJ, Marshall J. Photorefractive keratectomy: a technique for laser refractive surgery. *J Cataract Refract Surg*. 1988,14, 46-52.

[2] Pallikaris IG, Katsanevaki V.J., Kalyvianaki MI, Naoumidi II. Advances in subepithelial excimer refractive surgery techniques: Epi-LASIK. *Curr Opin Ophthalmol*, 2003, 14, 207-212.

[3] Thibos LN. The prospects for perfect vision. *J Refract Surg*, 2000, 16, S540-S546.

[4] Applegate RA. Limits to vision: can we do better than nature? *J Refract Surg*, 2000,16, S547-S551.

[5] Kanjani N, Jacob S, Agarwal A, Agarwal A, Agarwal S, Agarwal T, Doshi A, Doshi S. Wavefront- and topography-guided ablation in myopic eyes using Zyoptix. *J Cataract Refract Surg*, 2004, 30, 398-402.

[6] Roberts C. The cornea is not a piece of plastic. *J Refract Surg*, 2000,16, 407-409.

[7] Roberts C. Biomechanics of the cornea and wavefront-guided laser refractive surgery. *J Refract Surg*, 2002, 18, S589-S592.

[8] Netto MV, Mohan RR, Ambrosio R, Hutcheon AEK, Zieske JD,. Wilson SE. Wound Healing in the Cornea. A Review of Refractive Surgery Complications and New Prospects for Therapy. *Cornea*, 2005, 24, 509–522.

[9] Serrao S, Lombardo M. One-year results of photorefractive keratectomy with and without surface smoothing using the Technolas 217C Laser. *J Refract Surg*, 2004, 20, 444-449.

[10] Lombardo M, Serrao S. Smoothing of the ablated porcine corneas using the Technolas Keracor 217C and Nidek EC-5000 excimer lasers. *J Refract Surg*, 2004, 20, 450-453.

[11] Ginis HS, Katsanevaki VJ, Pallikaris IG. Influence of ablation parameters on refractive changes after phototerapeutic keratectomy. *J Refract Surg*, 2003, 19, 443-447.

[12] Lombardo M, De Santo MP, Lombardo G, Barberi R, Serrao S. Roughness of excimer laser ablated corneas with and without smoothing with atomic force microscopy. *J Refract Surg*, 2005, 21, 469-475.

[13] Binning G, Quate C, Gerber C. Atomic force microscope. *Phys Rev Lett*, 1986, 56, 930-939.

[14] Weiss RA, Liaw L-H L, Berns M, Amoils SP. Scanning electron microscopy comparison of corneal epithelial removal techniques before photorefractive keratectomy. *J Cataract Refract Surg*, 1999, 25, 1093-1096.

[15] Abrams GA, Goodman SL, Nealy PF, Franco M, Murphy CJ. Nanoscale topography of the basament membrane underlying the corneal epithelium of the rhesus macaque. *Cell Tissue Res*, 2000, 299, 39-46.

[16] Nogradi A, Hopp B, Revesz K, et al. Atomic force microscopic study of the human cornea following excimer laser keratectomy. *Exp Eye Res*, 2000, 70, 363-368.

[17] Taylor ST, Fields CR, Barker FM, et al. Effect of depth upon the smoothness of excimer laser corneal ablation. *Opt Vis Sci*, 1994, 71, 104-108.

[18] Lydataki S, Lesniewska E, Tsilimbaris MK, Panagopoulou S, Le Grimellec G., Pallikaris IG. Excimer laser ablated cornea observed by atomic force microscopy. *Single Mol*, 2002, 2-3, 141-147.

[19] Doughty MJ. On the evaluation of the corneal epithelial surface by scanning electron microscopy. *Optom Vis Sci*, 1990, 67, 735-756.

[20] Tsilimbaris MK, Lesniewska E, Lydataki S, Le Grimellec C, Goudonnet JP, Pallikaris IG. The use of atomic force microscopy for the observation of corneal epithelium surface. *Invest Ophthalmol Vis Sci*, 2000, 41, 680-686.

[21] Sinniah, K, Paauw, J, Ubels, J. Investigating live and fixed epithelial and fibroblast cells by atomic force microscopy. *Curr Eye Res*, 2002; 25, 61-68

[22] Damiano RE, Van Horn DL, Schultz RO. Trephination of donor corneal buttons: a scanning electron microscopic study. *Ann Ophthalmol*, 1978, 10, 479-485.

[23] Kerr-Muir MG, Trokel SL, Marshall J, Rothery S. Ultrastructural comparison of conventional surgical and argon fluoride excimer laser keratectomy. *Am J Ophthalmol*, 1987, 103, 448-453.

[24] Smith JR. A quantitative method for analysing AFM images of the outer surfaces of human hair, *J Microsc*, 1998, 191, 223-228.

[25] Williams D, Yoon GY, Porter J, Guirao A, Hofer H, Cox I. Visual benefit of correcting higher order aberrations of the eye. *J Refract Surg*, 2000, 16, S554-S559.

[26] Weber BA, Gan L, Fagerholm P. Wound healing response in the presence of stromal irregularities after excimer laser treatment. *Acta Ophthalmol Scand*, 2001, 79, 381-388.

[27] Møller-Pedersen T, Cavanagh HD, Petroll WM, Jester JV. Stromal wound healing explains refractive instability and haze development after photorefractive keratectomy. *Ophthalmology*, 2000, 107, 1235-1245.

[28] Van Horn SD, Hovanesian JA, Maloney RK. Effect of volatile compounds on excimer laser power delivery. *J Refract Surg*, 2002, 18, 524-528.

[29] Maldonado-Codina C, Morgan PB, Efron N. Thermal consequences of photorefractive keratectomy. *Cornea*, 2001, 20, 509-515.

[30] Trokel SL, Srinivasan R, Braren B. Excimer laser surgery of the cornea. *Am J Ophthalmol*, 1983, 96, 710-715.

[31] Braet F, Kalle WH, De Zanger RB, et al. Comparative atomic force and scanning electron microscopy: an investigation on fenestrated endothelial cells in vitro. *J Microsc*, 1996, 181, 10-17.

[32] Poletti G, Orsini F, Lenardi C, et al. A comparative study between AFM and SEM imaging on human scalp hair. *J Microsc*, 2003, 21, 249-255.

[33] Lombardo M, De Santo MP, Lombardo G, Barberi R, Serrao S. Atomic Force Microscopy analysis of normal and photoablated porcine corneas. *J Biomechanics*, 2006, 39, 2719-2724.

[34] Abrams GA, Bentley E, Nealey PF, Murphy CJ. Electron microscopy of the canine corneal basement membranes. *Cells Tissues Organs*, 2002, 170, 251-257.

[35] Hayashi, S, Osawa, T, Tohyama, K. Comparative observations on corneas, with special reference to Bowman's layer and Descemet's membrane in mammals and amphibians. *J Morphol*, 2002, 254, 247-258.

[36] Dalton BA, McFarland GA, Steele JG. Stimulation of epithelial tissue migration by certain porous topographies is independent of fluid flux. *J Biomed Mater Res*, 2001, 56, 83-92.

[37] Betney S, Morgan PB, Doyle SJ, Efron N. Corneal temperature changes during photorefractive keratectomy. *Cornea*, 1997, 16, 158-161.

[38] Puliafito CA, Steinert RF, Deutsch TF, Hillenkamp EJ, Dehm CM. Adler . Excimer laser ablation of the cornea and lens. *Ophthalmology*, 1985, 92, 741-748.

[39] Hahn DW, Ediger MN, Pettit GH. Dynamics of ablation plume particles generated during excimer laser corneal ablation. *Lasers Surg Med*, 1995, 16, 384-389.

[40] DeMali KA, Williams TR. Determination of the content of water in bovine corneas by differential scanning calorimetry and thermogravimetric analysis. *Ophthalmic Res*, 1994, 26, 105-109.

[41] Randleman JB, Loft ES, Banning CS, Lynn MJ, Stulting RD. Outcomes of wavefront-optimized surface ablation. *Ophthalmology*, 2007, 114, 983-988.